Supporting information for

Engineering interface structure between lead halide perovskite and copper phthalocyanine for efficient and stable perovskite solar cells

Young Chan Kim,[a,⊥] Tae-Youl Yang, [a,⊥] Nam Joong Jeon, [a] Jino Im,[a] Seunghun Jang,[a] Tae Joo Shin,[b] Hee-Won Shin,[c] Sol Kim,[d] Eunyeong Lee,[d] Sanghak Kim,[d] Jun Hong Noh,[a] Sang Il Seok*,[ae] and Jangwon Seo*,[a]

[a]Division of Advanced Materials, Korea Research Institute of Chemical Technology (KRICT), 141 Gajeong-Ro, Yuseong-Gu, Daejeon 305-600, South Korea

[b] Central Research Facilities, Ulsan National Institute of Science and Technology (UNIST), 50 UNIST-gil, Ulsan 44919, South Korea

[c] Department of Energy Science, School of Chemical Engineering, Sungkyunkwan University, Suwon 440-746, Korea

[d]Central Advanced Research & Engineering Institute, Hyundai Motor Company, 37 Cheoldoangmulgwan-ro, Uiwang-si, Gyeonggi-do, 16082, Korea

[e]School of Energy and Chemical Engineering, Ulsan National Institute of Science and Technology (UNIST), 50 UNIST-gil, Ulsan 44919, South Korea

[⊥]These authors contributed equally to this work *E-mail: jwseo@krict.re.kr and seoksi@krict.re.kr (seoksi@unist.ac.kr)

Device fabrication

F-doped SnO_2 (FTO, Pilkington, TEC8) substrate was cleaned in an ultrasonic bath containing detergents for 30 min and then a dense blocking layer of TiO_2 (60 nm, bl-TiO_2) was deposited onto the FTO by spray pyrolysis using a 20 mM titanium diisopropoxide bis(acetylacetonate) solution (Aldrich) at 450 °C. A 100-nm thin mesoporous (mp)-TiO_2 was spin-coated on top of the bl-TiO_2/FTO substrate at 1000 rpm for 50 s using home-made TiO_2 (~ 50 nm in particle size) pastes. Where, the pristine paste had been diluted in 2-methoxyethanol (1g / 5mL), and calcinated at 500 °C for 1 h in air which led to a thickness of about 100 nm. The $(FAPbI_3)_{0.85}(MAPbBr_3)_{0.15}$ perovskite solutions with small excess of PbI_2 were then coated onto the mp-TiO_2/bl-TiO_2/FTO substrate uniformly heated to ~80 °C by two consecutive spin-coating steps, at 1000 and 5000 rpm for 15 s and 10 s, respectively. During the second spin-coating step, 1 mL ethyl ether was poured onto the substrate. The 1.05M solution for $(FAPbI_3)_{0.85}(MAPbBr_3)_{0.15}$ perovskite was obtained by dissolving $NH_2CH=NH_2I$ (=FAI) and CH_3NH_3Br(=MABr) with PbI_2 and $PbBr_2$ in N-N-dimethylformamide(=DMF) and dimethylsulfoxide(=DMSO) =(6 : 1 v/v). The different inorganic-organic lead halide triiodide powders were prepared by precipitation using toluene at room temperature from the desired compositional solutions obtained by dissolving FAI and MABr powders with PbI_2 and $PbBr_2$ in 2-methoxyethanol. Then the substrate was dried on a hot plate at 100 °C for 10 min. A Spiro-OMeTAD (LUMTEC)/chlorobenzene (30 mg/ 1 ml) solution with an additive of 22.5 µl Li-bis(trifluoromethanesulfonyl) imide (Li-TFSI)/acetonitrile (170 mg/ 1 ml), 22.5µl 4-tert-butylpyridine (TBP)/acetonitrile (1ml / 1ml) and tris(2-(1H-pyrazol-1-yl)-4-tert-butylpyridine)-cobalt(III) tris(bis(trifluoromethylsulfonyl)imide:(FK209)/acetonitrile (150mg/1ml) was spin-coated on $(FAPbI_3)_{0.85}(MAPbBr_3)_{0.15}$/mp-$TiO_2$/bl-$TiO_2$/FTO substrate at 3000 rpm for 30 s. Also, the

CuPc (Sigma)/chlorobenzene (10mg/1ml) solution was prepared with an additive of 7.5 µl Li-TFSI/acetonitrile (170 mg/ 1 ml) and 7.5µl TBP/acetonitrile (1ml / 1ml). Finally, Au counter electrode was deposited by thermal evaporation. The active area of this electrode was fixed at 0.16 cm^2.

Characterizations and measurements

The morphologies of the perovskite film coated with or without CuPC and the prepared devices were investigated using FE-SEM (Tescan Mira 3 LMU FEG). The absorption spectra were obtained using a UV-visible spectrophotometer (Shimadzu UV 2550) in the wavelength range of 300 nm to 900 nm. The photovoltaic properties of the devices were measured using a solar simulator (Newport, Oriel Class A, 91195 A) with a source meter (Keithley 2420) at AM 1.5 G 100 mAcm^{-2} of illumination and a calibrated Si-reference cell certificated by NREL. The J–V curves of all the devices were measured by masking the active area using a metal mask with an area of 0.096 cm^2. The XRD spectra were measured using a Rigaku Smart Lab X-ray diffractometer to identify the crystal phase of the prepared films. Grazing incidence X-ray diffraction (GIXD) measurements were conducted at PLS-II 6D UNIST-PAL beamline of Pohang Accelerator Laboratory in Korea. The X-rays coming from the bending magnet are monochromated (wavelength λ = 1.069 Å) using a double crystal monochromator and focused both horizontally and vertically (120 (V) x 150 (H) µm2 in FWHM @ sample position) using the sagittal Si(111) crystal and toroidal mirror. The vacuum GIXD sample chamber is equipped with a 5-axis motorized stage for the fine sample alignment. The incidence angle of X-ray beam was set to 0.15º, which is close to the critical angle of perovskites. Two-dimensional GIXD patterns were recorded with a 2D CCD detector (Rayonix MX 225-HS, USA). Diffraction angles were calibrated by a pre-calibrated sucrose (Monoclinic, P21, a = 10.8631 Å, b = 8.7044 Å, c = 7.7624 Å, b = 102.938o) [R. C.

Hynes and Y. Le Page, J. Appl. Cryst. 24 (1991) 352–354] and the sample-to-detector distance was about 246.4 mm. For Raman analysis, CuPC/perovskite composite powder was collected by mixing a tiny powder of FAPbI3 into a chlorobenzene solution of CuPC, followed by filtration and drying process. A Bruker Senterra Raman spectroscope with a 532 nm laser line was used at room temperature. Adhesive tapes were attached on the top of devices where surface of HTMs (CuPC, Spiro-OMeTAD, and PTAA, repectively) is exposed and removed the tape by pulling it off rapidly back upon itself at as close to an angle of 180° as possible. Scotch® Magic™ tape or Scotch® double side tape was used as an adhesive tape. Time-resolved photoluminescence (TRPL) decay profiles were measured at 780 nm with 550 nm excitation of OPO laser system (EKSPLA, NT 342A-10-AW). The pulse energy was strongly attenuated to less than 1μJ, in order to avoid nonlinear effect such as exciton-exciton annihilation. Emissions from samples were collected by a monochromator (Princeton Instruments, SP2150) equipped with a PMT (Hamamatsu, H10721-20). The output signal from a PMT was recorded with a 500 MHz digital oscilloscope (Agilent, DSO-X 3054A).

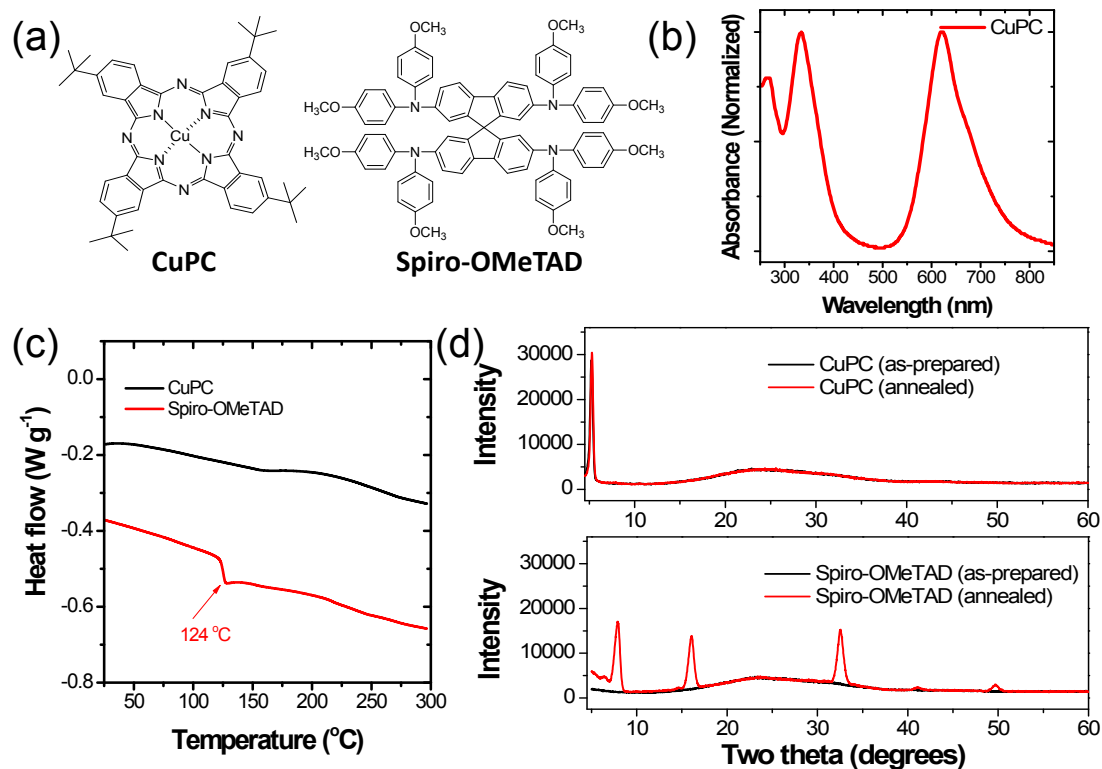**Thermal stability of HTMs**

Figure S1. CuPC vs Spiro-OMeTAD. (a) Molecular structure of CuPC and Spiro-OMeTAD. (b) UV-vis absorption spectrum of CuPC film state. (c) DSC trace of CuPC and Spiro-OMeTAD (2nd cooling at 10 ˚C/min) (d) X-ray diffraction patterns of CuPC and Spiro-OMeTAD in film state before (black color) and after (red color) annealing at 130 ˚C for 30 min.
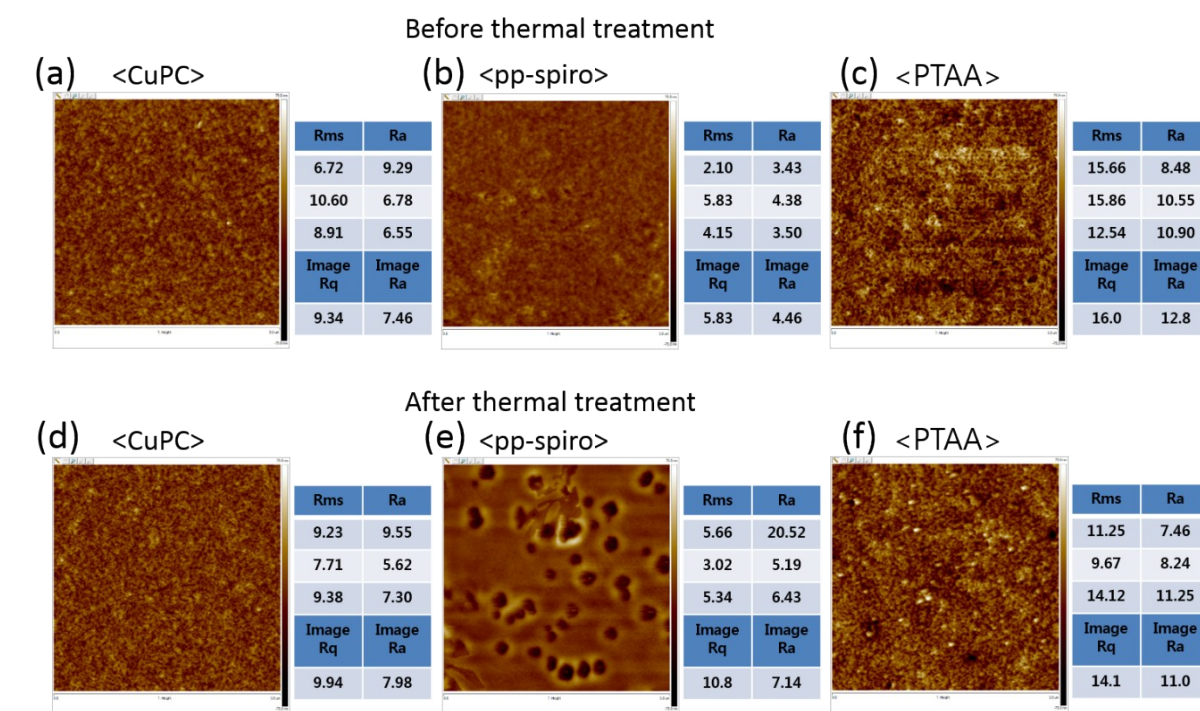
Before thermal treatment

(a) <CuPC>

Rms	Ra
6.72	9.29
10.60	6.78
8.91	6.55
Image Rq	Image Ra
9.34	7.46

(b) <pp-spiro>

Rms	Ra
2.10	3.43
5.83	4.38
4.15	3.50
Image Rq	Image Ra
5.83	4.46

(c) <PTAA>

Rms	Ra
15.66	8.48
15.86	10.55
12.54	10.90
Image Rq	Image Ra
16.0	12.8

After thermal treatment

(d) <CuPC>

Rms	Ra
9.23	9.55
7.71	5.62
9.38	7.30
Image Rq	Image Ra
9.94	7.98

(e) <pp-spiro>

Rms	Ra
5.66	20.52
3.02	5.19
5.34	6.43
Image Rq	Image Ra
10.8	7.14

(f) <PTAA>

Rms	Ra
11.25	7.46
9.67	8.24
14.12	11.25
Image Rq	Image Ra
14.1	11.0

Figure S2. AFM images for the as-prepared films of CuPC (a), Spiro-OMeTAD (b), and (c) PTAA on top of the perovskite film. AFM images for the annealed films (at 130 ˚C for 30 min in nitrogen-filled glove box) of CuPC (d), Spiro-OMeTAD (e), and (f) PTAA on top of the perovskite film. The scale is 3 μm.
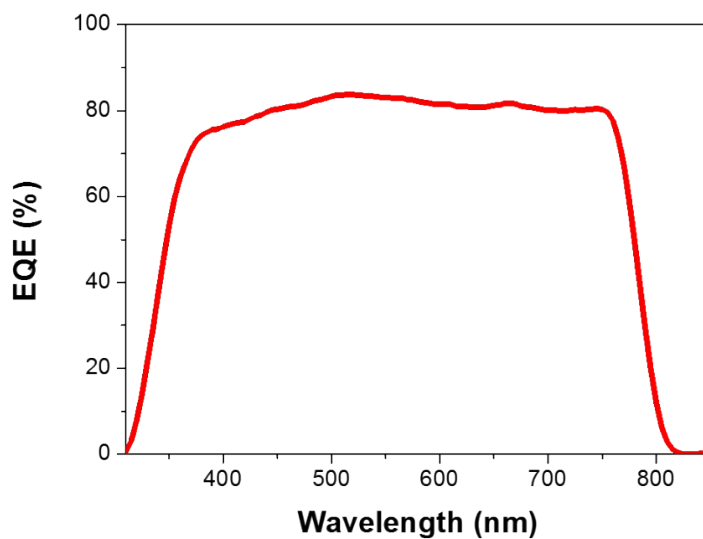
Performance of devices

Figure S3. External quantum efficiency measurements of a CuPC-applied perovskite solar cell.
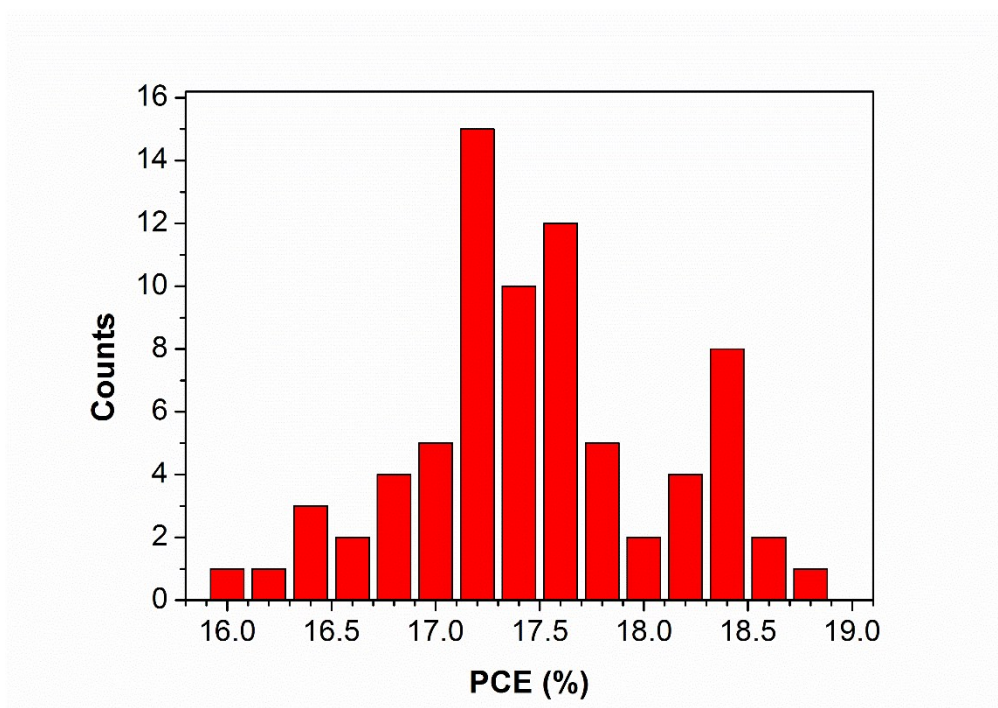

Figure S4. Distribution of power conversion efficiencies for devices with CuPC.
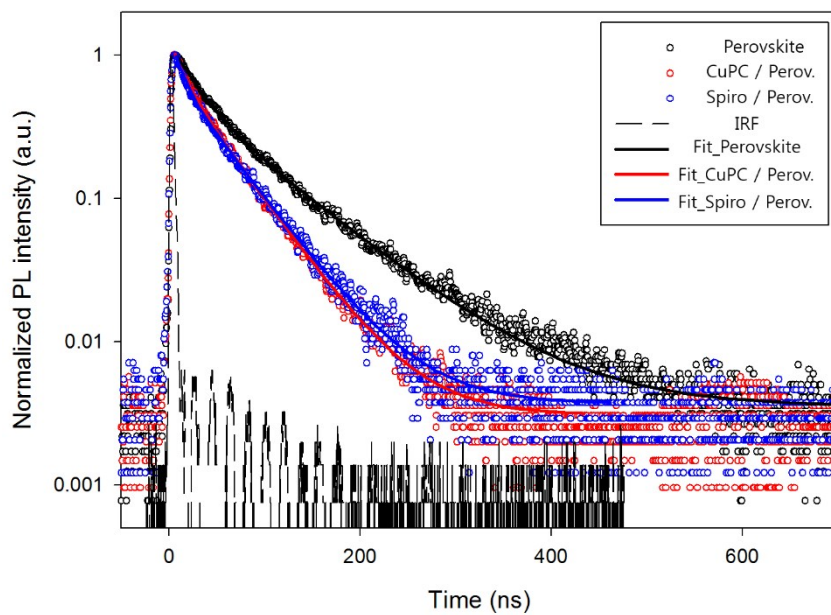
Figure S5. Time-resolved photoluminescence (TRPL) spectra for a perovskite film (black), a Spiro-OMeTAD / perovskite bilayer film (blue), and a CuPC / perovskite bilayer film (red).
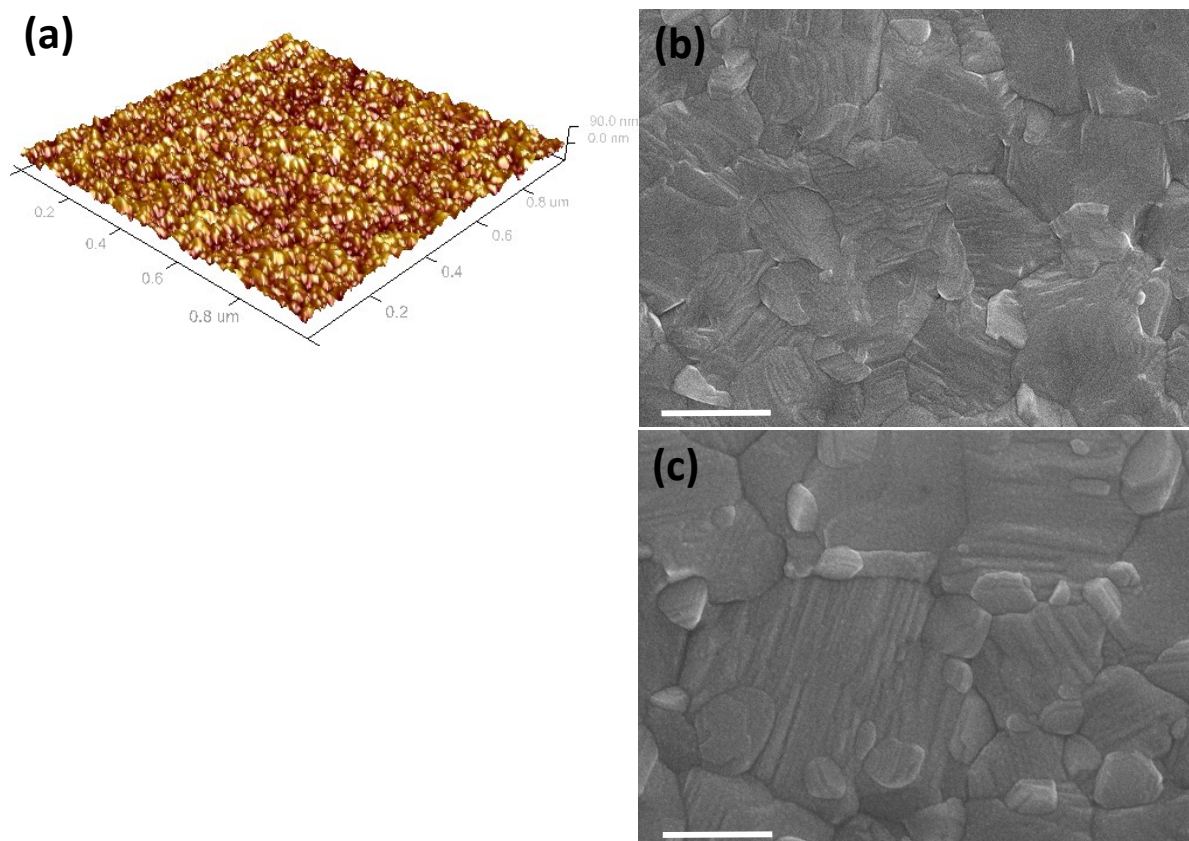
AFM image / Facet SEM images

Figure S6. (a) AFM image for the perovskite film prepared from Figure 3 and (b) (c) their top view SEM images. The scale bar is 500 nm and 100 nm for b and c, respectively.
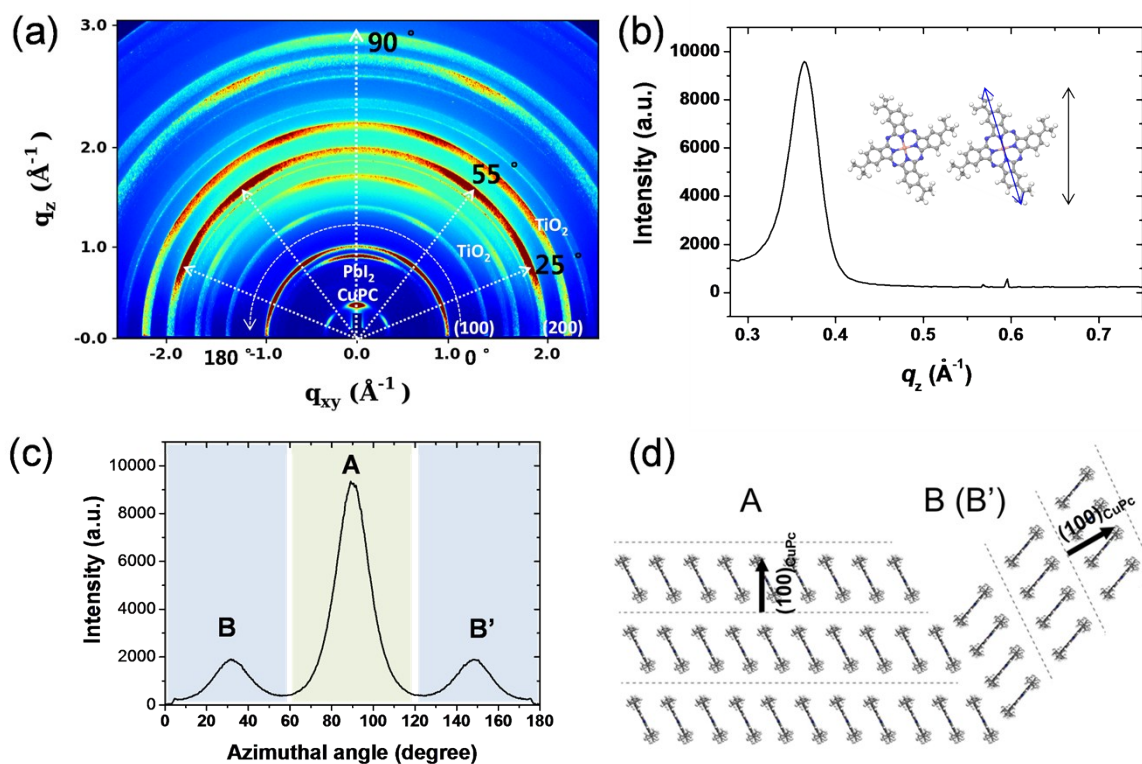
CuPC arrangement

Figure S7. (a) 2D GIWAXS image of FTO/d-TiO$_2$/mp-TiO$_2$/perovskite/CuPC. (as the same in Figure 3) (b) Radial line profiles at 90 °. Inset shows the molecular structure of CuPC and the calculated distances (of the extended molecular length (blue arrow) and layer spacing (black arrow)). (c) Intensity plots as a function of azimuthal angle along the ring at q=0.37 Å^{-1}, assigned to CuPC film. Inset shows multiple orientations (A, B, and B') of CuPC. (d) The proposed schematic of molecular arrangement of CuPC at the interface of the perovskite film.

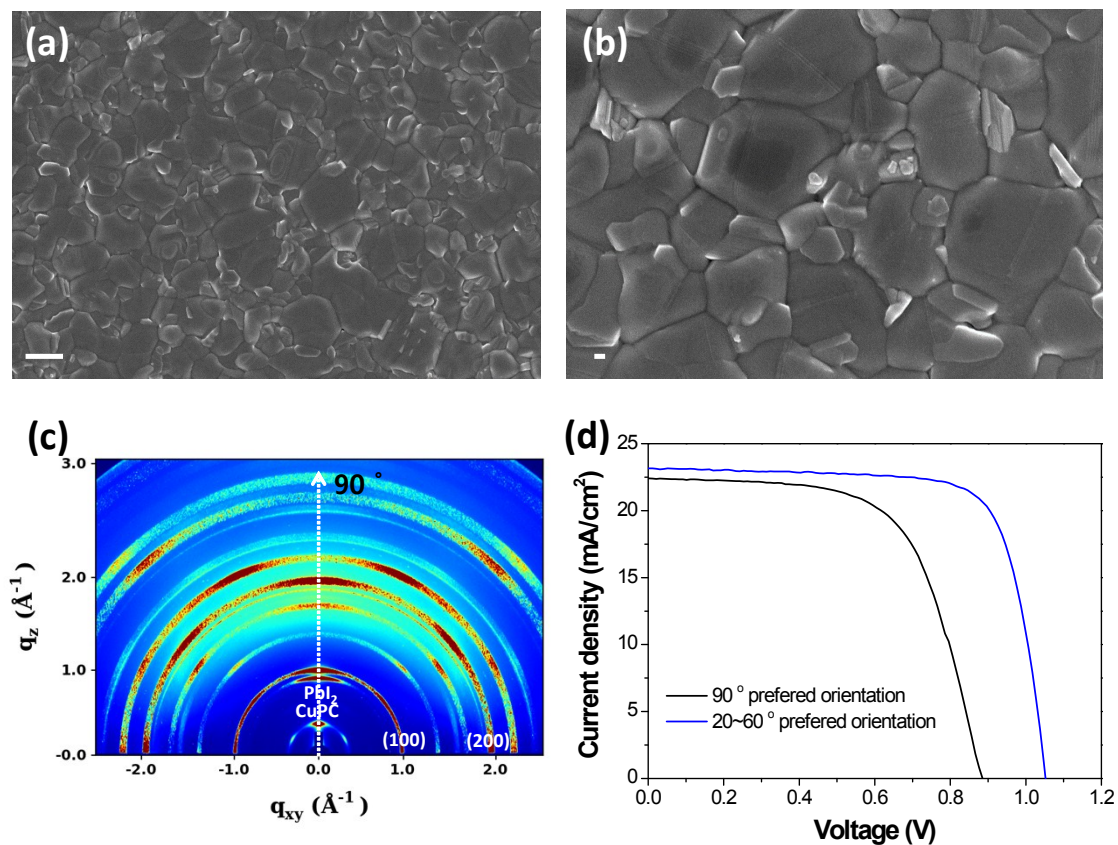**Cl-induced perovskite film and J-V curve comparison**

Figure S8. (a) Top view SEM image for Cl-induced perovskite film [reference: J. Qing *et. al. org. electronics* (2016), 38, 144-149.] and (b) its magnified image. The scale bar is 1 μm and 100 nm for a and b, respectively. (c) 2D-GIWAXS images of Cl-induced perovskite film, (d) J-V curves for the devices employing Cl-induced perovkite film and the perovskite film used in this work (from Figure 3).

GIWAXS data as a function of incident angle

The relation between the penetration depth (Λ) and the incident angle is described by

$$\Lambda = \frac{\sqrt{2}\left(\frac{\lambda}{4\pi}\right)}{\left\{\sqrt{(\alpha^2-\alpha_c^2)^2+(2\beta)^2}-(\alpha^2-\alpha_c^2)\right\}^{\frac{1}{2}}} \qquad \beta = \frac{\lambda\mu}{4\pi}$$
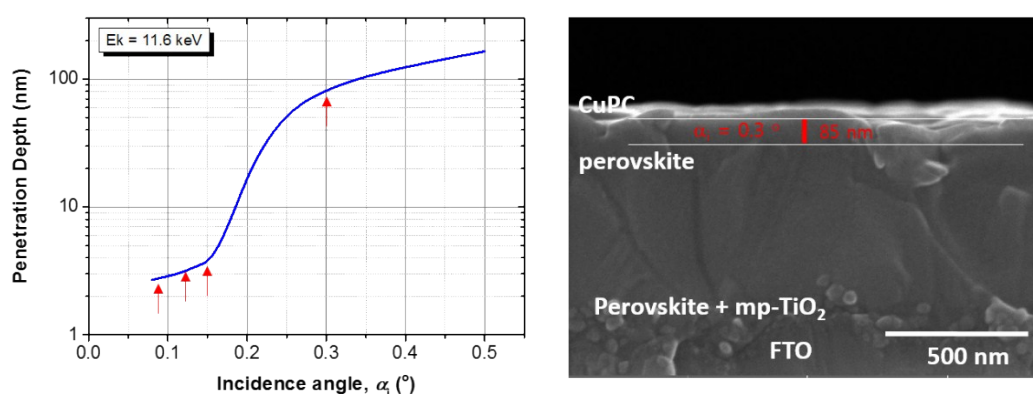

Figure S9. Penetration depth for the perovskite layer as a function of incident angle. In SEM image interaction thickness for incident angle of 0.3 ˚ is marked.

We did GIWAXS measurements using various incident angles from 0.08 ˚ to 0.5 ˚.
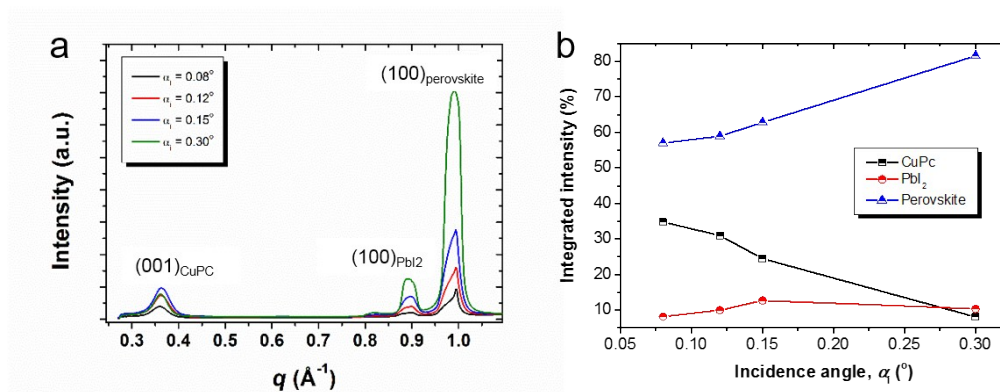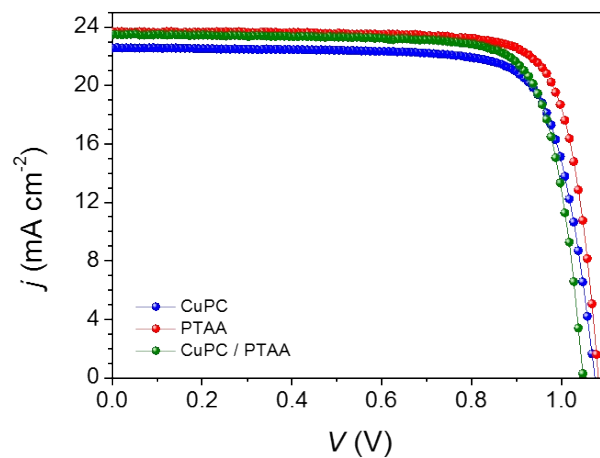

Figure S10. (a) GIWAXS spectrum at the angle of 90 ˚ with variation of incident angles. (b) Integrated intensity of scattering peaks for (001)CuPC (black), (100)PbI$_2$ (red), and (100)perovskite (blue) as a function of incident angles.

	Voc (V)	Jsc (mA/Cm^2)	Fill factor (%)	PCE (%)
CuPC	1.07	22.6	77.5	18.8
PTAA	1.08	23.7	80.3	20.5
CuPC / PTAA	1.04	23.5	79.0	19.4

Figure S11. PCE of PSCs with using CuPC, PTAA, and the double layer of CuPC and PTAA as a HTM. To prepare the double layer of CuPC (~thin layer) and PTAA, PTAA solution in toluene was additionally spin-coated on top of CuPC-coated device.

Thermal cycling test in dry air

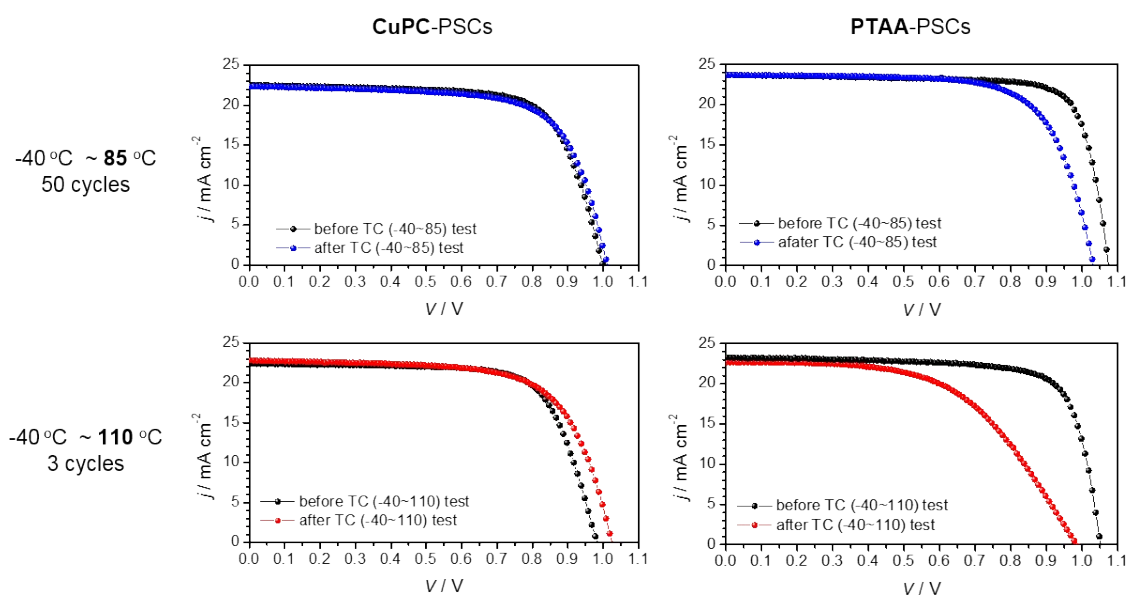|	Test 1	Test 2
Temperature range	-40 ~ 85 $^{\circ}$C	-40 ~ 110 $^{\circ}$C
Ramp rate	1 $^{\circ}$C / min	1.8 $^{\circ}$C / min
Dwell time @ max. & min. temperature	10 min	60 min
Number of cycles	50	3

* for non-encapsulated devices

Figure S12. Power conversion efficiencies of CuPC-PSCs and PTAA-PSCs without encapsulation before and after the thermal cycling test with the temperature range of -40 $^{\circ}$C ~ 85 $^{\circ}$C and -40 $^{\circ}$C ~ 110 $^{\circ}$C.